On the dynamic response of shallow foundations in saturated soils

Giuseppe Lombardi [i)], Davide Noè Gorini [ii)] and Luigi Callisto [iii)]

i) Ph.D Student, Department of Structural and Geotechnical Engineering, Sapienza University of Rome, Via Eudossiana, 18 , Rome 00184, Italy.
ii) Postdoctoral researcher, Department of Structural and Geotechnical Engineering, Sapienza University of Rome, Via Eudossiana, 18 , Rome 00184, Italy.
iii) Professor, Department of Structural and Geotechnical Engineering Sapienza University of Rome, Via Eudossiana, 18 , Rome 00184, Italy.

ABSTRACT

In recent years, the development of macroelement approaches to include the macroscopic nonlinear response of soil-foundation systems in the assessment of structures is receiving an increasing interest by virtue of the minimal computational effort required. However, existing formulations commonly neglect any undrained or partly drained soil behaviour, that may be crucially important for simulating the response under dynamic loading. The present study provides an insight into the effects of the hydro-mechanical coupling of the soil on the macroscopic multiaxial cyclic response of shallow foundations. This is accomplished through a series of nonlinear transient analyses on a fully coupled soil-foundation numerical model implemented in OpenSees, providing an explicit description of the pore water pressure build-up induced by the nonlinear soil behaviour. The numerical study explores different assumptions for the hydraulic regime, from drained to undrained conditions. The effect of the volumetric-deviatoric coupling on the cyclic response of the reference foundation is examined, highlighting the key role played by the drainage conditions on the stiffness and dissipative features of the foundation system. The effect of non-linearity on the above effects is discussed and interpreted in terms of degradation of the system response at the macro scale.

Keywords: nonlinear soil-foundation interaction, cyclic loading, excess pore water pressure, volumetric-deviatoric coupling, OpenSees

1 INTRODUCTION

The cyclic response of shallow foundations on saturated soils is intimately related to the development of excess pore water pressure. During strong motion, an undrained soil response amplifies the displacements of the foundation occurring under dynamic loading (Liu & Dobry, 1997, Dashti et al., 2010, Karamitros et al., 2013).

Despite the evidence gained over the years, there is still the lack of standardized numerical procedures for the prompt evaluation of the pore water pressure-related effects at the scale of the geotechnical system. Consequently, the hydro-mechanical coupling of the cyclic response of shallow foundations is typically neglected in design and assessment of ordinary structures. For instance, the macroelement approach (Roscoe & Schofield, 1956, Nova & Montrasio, 1991, Cremer et al., 2002) was seen to be quite effective in simulating the multiaxial response of geotechnical systems under dynamic conditions (Gorini & Callisto, 2022, Gorini et al., 2023a, Gorini & Callisto, 2023b), assuming however a drained response. The inclusion of a more realistic undrained response would entail instead the implementation of very demanding numerical models that can be warranted only for structures of major importance.

In light of the above, the present study aims at highlighting key aspects affecting the cyclic response of shallow foundations in saturated soils at the macro-scale, as a preliminary step for the extension of nonlinear macroelement approaches to the simulation of the dynamic soil-foundation interaction. These macroscopic effects are quantified by means of the fully coupled modelling of the soil-foundation system recounted in the following.

2 NUMERICAL MODEL

The coupled, hydro-mechanical response of the soil-foundation system was investigated through the three-dimensional numerical model in Figure 1, that was implemented in the finite-element analysis framework OpenSees (McKenna et al., 2010). It consists of a square footing, with a width b = 1.5 m and a thickness h = 0.5 m, resting on a sandy soil deposit (average shear wave velocity V_s = 156 m/s). The small-strain shear modulus G_0 increases with the mean effective pressure p’

according to the following power law:

$$G_0 = G_r \left(\frac{p'}{p'_r} \right)^d \qquad (1)$$

The ground water table is coincident with the ground level. A thin layer of solid elements with reduced strength parameters was interposed between the foundation and the soil to reproduce the stress concentration in the soil in proximity to the contact (interface elements in Fig. 1). As a result of a preliminary sensitivity analysis, the extension of the soil domain was set to avoid significant boundary effects. In order to reduce computation time, only half of the domain was modelled, exploiting the symmetry of the problem (see Fig. 1).

The domain discretization was performed through a parametric mesh tool, implemented in Matlab. The soil domain is discretized as 7680 8-nodes hexahedral SSPbrickUP-type elements (McGann et al., 2015). The behaviour of the soil and the interface elements was described with the multi-yield surface model developed by Yang et al. (2003), commonly denoted as PDMY, that is an elastic-plastic constitutive law with kinematic hardening. Model parameters are reported in Table 1, calibrated on the basis of a previous study (Gallese et al., 2023) concerning a coarse-grained soil with a substantially contractive behaviour.

The foundation is discretized with 4-noded ShellMITC4-type quadrilateral elements (Dvorkin & Bathe, 1984), exhibiting a linear elastic behaviour.

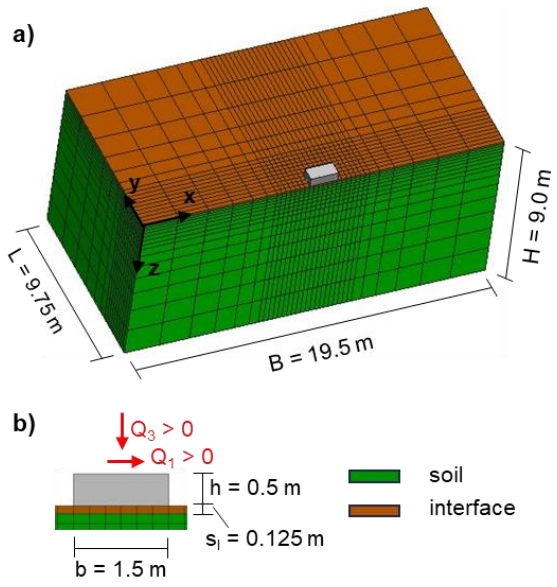

Figure 1. a) Mesh of the soil-foundation model implemented in OpenSees and b) detail of the soil-foundation contact.

The base of the model was restrained, whilst the motion of the nodes along the lateral boundaries was impeded in the respective normal direction. The numerical simulations were implemented in OpenSees as transient analyses in the time domain. The use of parallel computing, obtained through the interpreter OpenSeesSP (McKenna & Fenves, 2008), was needed to get reasonable computation times. Some of the analyses were carried out using the supercomputing resources at the Texas Advanced Computing Centre (Rathje et al., 2017).

Table 1. PDMY parameters for soil and interface.

Variables	Description	Soil	Interface
ρ (Mg/m^3)	Soil mass density	2.039	2.039
ν (-)	Poisson's coefficient	0.31	0.31
G_r (kPa)	elastic shear modulus	9.5×10^4	9.5×10^4
ϕ_{cs} (°)	friction angle	33	22.2
p'_r (kPa)	reference pressure	101.0	101.0
d (-)	pressure depend coefficient	0.5	0.5
γ_{max} (-)	peak shear strain	0.1	0.1
ϕ_{PTL} (°)	phase transformation angle	29.7	17.2
c_1 (-)	contraction parameter	0.07	0.07
d_1 (-)	dilation parameter	0.04	0.04
d_2 (-)	dilation parameter	2	2
N (-)	number of yield surfaces	30	30

3 MACROSCOPIC RESPONSE

As a first step to the development of a macro-element, the one-dimensional macroscopic response of the foundation to cyclic loading was explored in the horizontal direction only, under a constant value of the vertical force component. Cyclic, force-controlled loading sequences were applied to the foundation in a quasi-static manner, adopting a loading frequency of 0.1 Hz, sufficiently low to inhibit any inertial effect. In each sequence the load was applied in two stages, as depicted in Figure 2: i) a vertical load, Q_3, was applied under drained conditions, up to a value of about 30 % of the vertical bearing capacity of the foundation; this was followed by a small unloading stage; ii) a horizontal load, Q_1, was applied cyclically, according to the pseudo-harmonic function depicted in Fig. 2b that has a gradual increase and decrease of the amplitude at the first and last cycle, respectively.

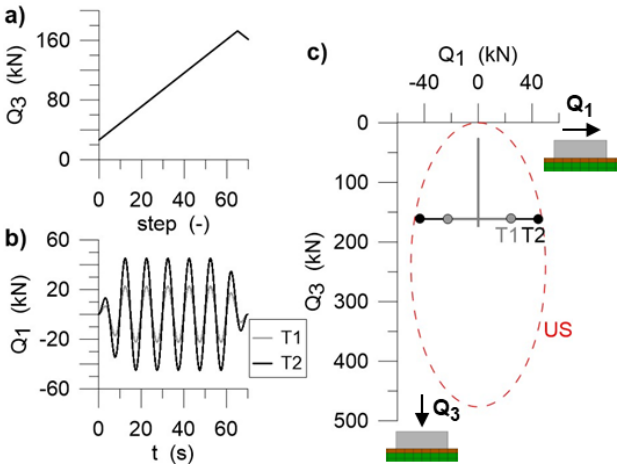

Figure 2. a) Initial drained loading phase, b) cyclic load phase, c) representation of the load paths in the Q_1-Q_3 load space, together with a schematic view of the ultimate limit curve (US).

In this cyclic loading stage, both drained (DC) and undrained conditions were considered, modifying the permeability of the soil. In turn, the undrained calculation was carried out with two different constitutive assumptions: the ordinary response of the constitutive model, which simulates a coupled volumetric-deviatoric response (UCC), and a modified constitutive response in which the volumetric-deviatoric coupling was inhibited (UCD) by setting the parameters c_1, d_1 and d_2 of the PDMY equal to zero.

For each case, two load amplitudes were examined, as shown in Fig. 2, corresponding to medium (T1) and high (T2) level of the mobilized resistance of the geotechnical system in the horizontal direction. Figure 2c shows as a reference the drained ultimate limit state locus (US) for the foundation, that was obtained with pushover analyses omitted here.

3.1 Response at moderate loading amplitude

Figure 3a illustrates, for sequence T1, the horizontal force-displacement relationship obtained in the 3rd and 6th loading cycle computed for the DC, UCC and UCD cases, whereas the evolution with the number of cycles N_{cyc} of the respective vertical displacements q_3 are shown in Figure 3b. For this loading amplitude the cyclic response of the foundation is only marginally influenced by drainage conditions: compared to the drained response, undrained conditions produce a negligible decrement of the secant stiffness. However, Figure 3.b indicates a certain accumulation of the settlements, with an increase of about 17%.

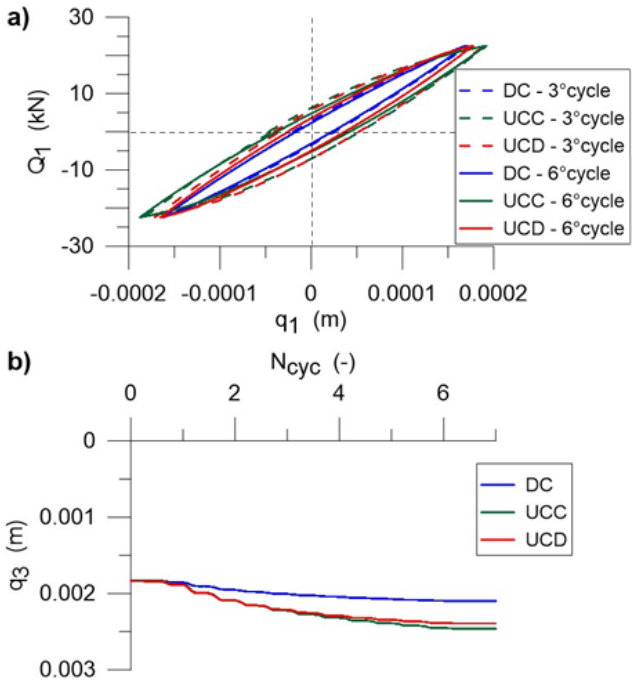

Figure 3. Comparison between the DC, UCC and UCD cases in terms of a) horizontal force-deformation relationship of the foundation in correspondence of the 3rd and 6th cycle, and b) time history of the vertical displacement for sequence T1.

At the macro-scale this evidences a more significant directional coupling of the foundation, that at the meso-scale should be ascribed to the undrained soil condition, but not to the volumetric-deviatoric coupling, that for the UCD condition is inhibited (compare UCC and UCD in Fig. 3). For this loading amplitude, both the drained and undrained responses of the foundation do not show any significant degradation effects, as a further proof that the volumetric-deviatoric behaviour is not at stake here.

Figure 4 quantifies the macroscopic stiffness and energy dissipation at this moderate loading amplitude, where the secant stiffness H_{11} was evaluated as the ratio of Q_1 and q_1 peaks at each cycle and the damping ratio ξ_{11} was computed from the area of the force-displacement cycles. The cases UCC and UCD present a moderate increase of ξ_{11} with respect to DC, in the range of 4% to 6%, marginally varying with the number of cycles.

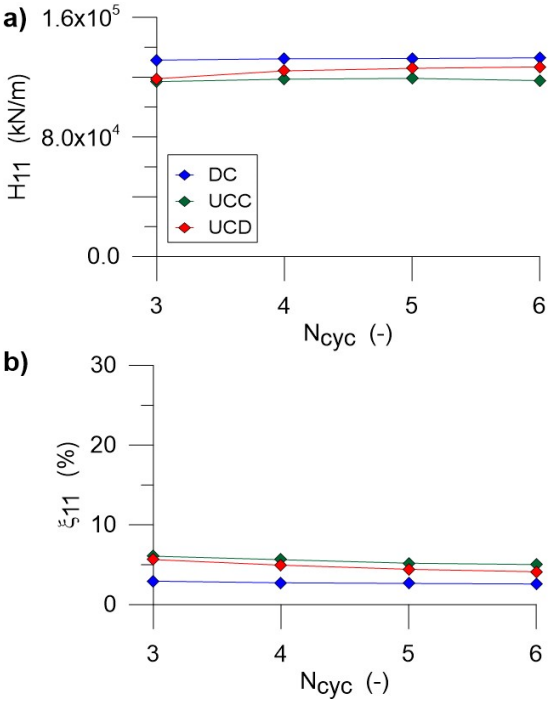

Figure 4. Evolution of a) the horizontal stiffness and b) the equivalent damping ratio with the number of cycle for test No. T1.

3.2 Response at high loading amplitude

The response to sequence T2 is reported in Figures 5 and 6, considering the same output quantities discussed in Section 3.1. At this larger amplitude the drainage conditions affect profoundly the macro-response of the foundation. Figure 6 shows that the secant stiffness H_{11} undergoes a progressive reduction as the number of cycles increase. This degradation has an effect on the directional coupling of the response, as the foundation settlements accumulate much more markedly that in the drained DC case (Figure 5.b).

It is interesting to comment in some detail the force-displacement cycles, that are depicted in Figure 5.a for

the 3rd and the 6th cycles, for the different drainage conditions. The most evident effect is that degradation is a direct effect of the volumetric-deviatoric coupling. This can be seen by comparing the two cycles drawn for the UCC case.

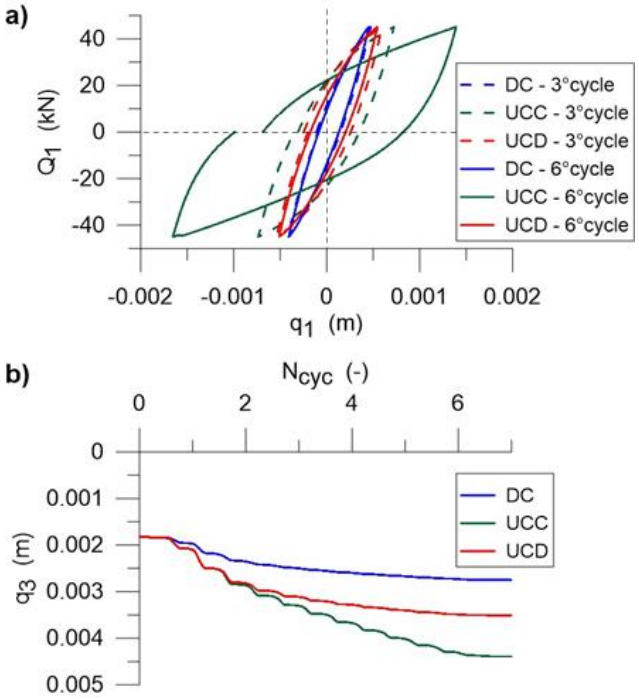

Figure 5. Comparison between the DC, UCC and UCD cases in terms of a) horizontal force-deformation relationship of the foundation in correspondence of the 3rd and 6th loading cycle, and b) time history of the vertical displacement for test T2.

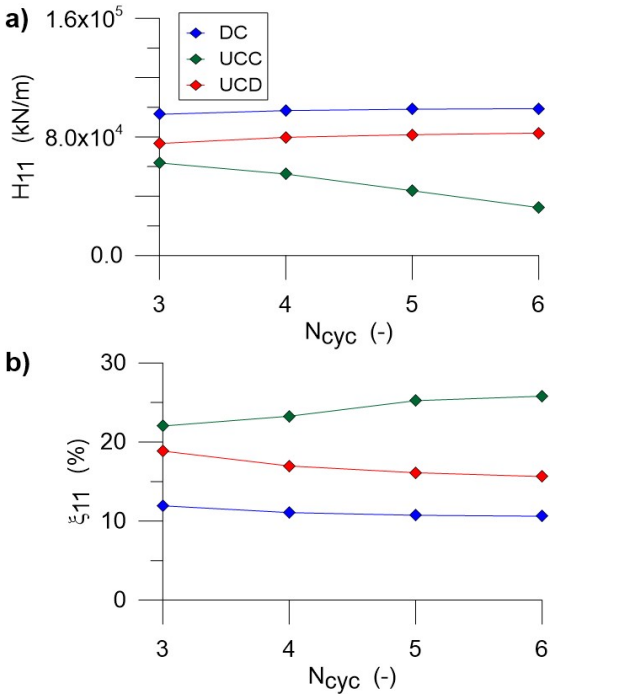

Figure 6. Evolution of a) the horizontal stiffness and b) the equivalent damping ratio with the number of cycle for test No. T2.

If compared with the drained (DC) case, an undrained response with no volumetric coupling (UCD) produces a smaller secant stiffness and a larger damping, but this effect is stable, in the sense that it does not evolve with the number of cycles, N_{cyc}. This is also visible from the variation of the vertical displacements with N_{cyc} (Figure 5.b) and from the evolution of the secant stiffness and the damping ratio with the load cycles (Figure 6).

As a general comment, the effect of the undrained condition on the foundation settlements can be regarded as resulting from two separate components: the impeded drainage, producing a constant increase in settlement, and the volumetric-deviatoric coupling producing a progressive deterioration of the system response. A further effect, evident in Figure 6.a, is that degradation also modifies the shape of the force-displacement cycles, in that it is seen to produce along the last cycle a certain increase of the tangent stiffness of the macro-response, that can be ascribed to a reduction of the amount of volumetric-deviatoric coupling with increasing plastic strains.

Figure 7 depicts the stress paths in the *q*-*p*' space (deviatoric stress vs mean effective stress) in two scrutiny gauss points at a depth z = *b*/2, located along the centreline (Figure 7a) and the edge (Figure 7b) of the foundation. In addition, Figures 8a,b show the corresponding evolution of the excess pore water pressure generated by the changes in the deviatoric stress $\Delta u_q = \Delta u - \Delta p$ as N_{cyc} increase, where Δu is the total excess pore water pressure.

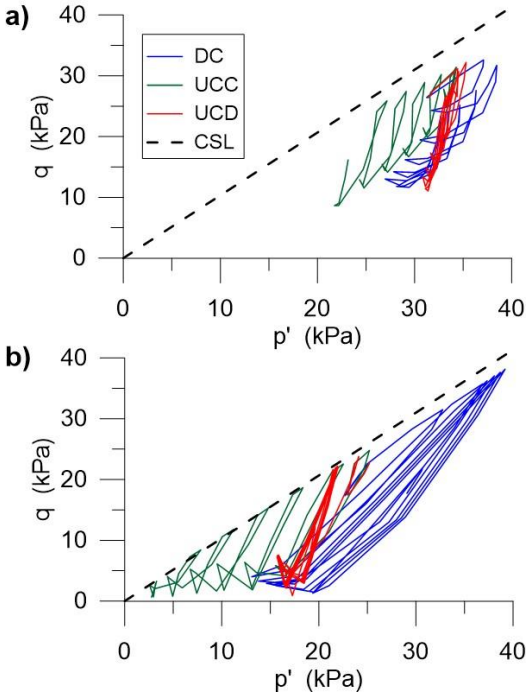

Figure 7. Sequence No. 3: responses of a soil element below the centre of the foundation at a depth of b/2 (a) and one along the edge at the same depth (b), in terms of paths in the stress invariants space.

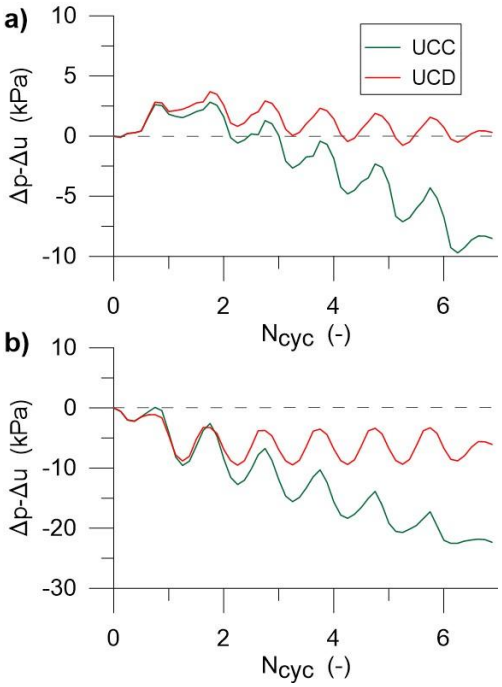

Figure 8. Sequence No. 3: responses of a soil element below the centre of the foundation at a depth of b/2 (a) and one along the edge at the same depth (b), in terms of evolution of the deviatoric-like excess pore water pressure Δu_q with the number of cycles.

For the UCD case, in ideally undrained conditions Δu_q should be equal to zero, and the stress paths in the q-p' plane should be vertical. The values of Δu_q computed for the UCD case in the analysis are due to the proximity of the soil surface, which acts as a draining boundary and allows some minor drainage to occur in the selects soil elements.

For the UCC case, Figures 8 indicates that for the large loading amplitude the primary contribution to the variation of the pore water pressure is given by the deviatoric part of the stress state that produces an accumulation of Δu_q, with stress paths veering towards the origin of the effective stress plane and a consequent significant reduction of the available soil strength. This tendency is more accentuated along the foundation edge, where cyclic variations of the deviator stress q prevail. Hence the degradation of the macroscopic response illustrated in Figure 5 can be directly related to the accumulation of excess pore water pressures generated by variations of the deviatoric stress.

5 CONCLUSIONS

The increasing attention towards soil-foundation interaction in the design and assessment of structures under dynamic loading requires practice-oriented numerical tools capable to include in a structural analysis a lumped macroscopic behaviour of the soil-foundation system. The study presented in this paper evidenced important features of the macroscopic response that derive from the hydro-mechanical coupling of the mechanical behaviour of saturated soils. These features may be incorporated into the current macroelement approaches, to produce a realistic prediction of the foundation behaviour under undrained conditions.

The numerical analyses shed the light on some dominant factors characterizing the undrained response of soil-foundation systems: i) the negligible effect of drainage conditions from low to medium loading amplitudes; ii) the substantial alteration of the stiffness and dissipative features of the geotechnical system for large amplitudes of the external loads, that implies cycle-dependency, with an increasing degradation of the mechanical response.

6 REFERENCIES

1) Cremer, C., Pecker, A., & Davenne, L. (2002). Modelling of nonlinear dynamic behaviour of a shallow strip foundation with macro-element. Journal of Earthquake Engineering, 6(02), 175-211.
2) Dashti, S., Bray, J. D., Pestana, J. M., Riemer, M., & Wilson, D. (2010). Mechanisms of seismically induced settlement of buildings with shallow foundations on liquefiable soil. Journal of geotechnical and geoenvironmental engineering, 136(1), 151-164.
3) Dvorkin, E. N., & Bathe, K. J. (1984). A continuum mechanics based four-node shell element for general non-linear analysis. Engineering computations, 1(1), 77-88.
4) Gallese, D., Noè Gorini, D., & Callisto, L. (2023). A nonlinear static analysis for the seismic design of single-span integral abutment bridges. Géotechnique, 1-40.
5) Gorini, D. N., & Callisto, L. (2022, August). A class of thermodynamic inertial macroelements for soil-structure interaction. In Conference on Performance-based Design in Earthquake. Geotechnical Engineering (pp. 1095-1102). Cham: Springer International Publishing.
6) Gorini, D. N., Callisto, L., Whittle, A. J., & Sessa, S. (2023a). A multiaxial inertial macroelement for bridge abutments. International Journal for Numerical and Analytical Methods in Geomechanics, 47(5), 793-816.
7) Gorini, D. N., & Callisto, L. (2023b). A multiaxial inertial macroelement for deep foundations. Computers and Geotechnics, 155, 105222.
8) Karamitros, D. K., Bouckovalas, G. D., Chaloulos, Y. K., & Andrianopoulos, K. I. (2013). Numerical analysis of liquefaction-induced bearing capacity degradation of shallow foundations on a two-layered soil profile. Soil Dynamics and Earthquake Engineering, 44, 90-101.
9) Liu, L., & Dobry, R. (1997). Seismic response of shallow foundation on liquefiable sand. Journal of geotechnical and geoenvironmental engineering, 123(6), 557-567.
10) MATLAB. Version R2023a. The MathWorks Inc., Natick, Massachusetts, 2023. URL https://www.mathworks.com.
11) McGann, C. R., Arduino, P., and Mackenzie-Helnwein, P. (2015). "A stabilized single-point finite element formulation for three-dimensional dynamic analysis of saturated soils," Computers and Geotechnics 66:126-141.
12) McKenna, F., Scott, M. H., & Fenves, G. L. (2010). Nonlinear finite-element analysis software architecture using object composition. Journal of Computing in Civil Engineering, 24(1), 95-107.
13) McKenna, F., & Fenves, G. L. (2008). Using the OpenSees interpreter on parallel computers. Network for earthquake engineering simulations.
14) Nova, R., & Montrasio, L. (1991). Settlements of shallow foundations on sand. Géotechnique, 41(2), 243-256.

15) Rathje, E., Dawson, C. Padgett, J.E., Pinelli, J.-P., Stanzione, D., Adair, A., Arduino, P., Brandenberg, S.J., Cockerill, T., Dey, C., Esteva, M., Haan, Jr., F.L., Hanlon, M., Kareem, A., Lowes, L., Mock, S., and Mosqueda, G. (2017): DesignSafe: A New Cyberinfrastructure for Natural Hazards Engineering. ASCE Natural Hazards Review,
16) Roscoe, K. & Schofield, A. (1956). The stability of short pier foundations on sand, discussion. Br. Welding J. 3, No. 8, 343–354.
17) Yang, Z., Elgamal, A., & Parra, E. (2003). Computational model for cyclic mobility and associated shear deformation. Journal of Geotechnical and Geoenvironmental Engineering, 129(12), 1119-1127.